Article

Cell Reports

IκB Kinase ε Is an NFATc1 Kinase that Inhibits T Cell Immune Response

Graphical Abstract

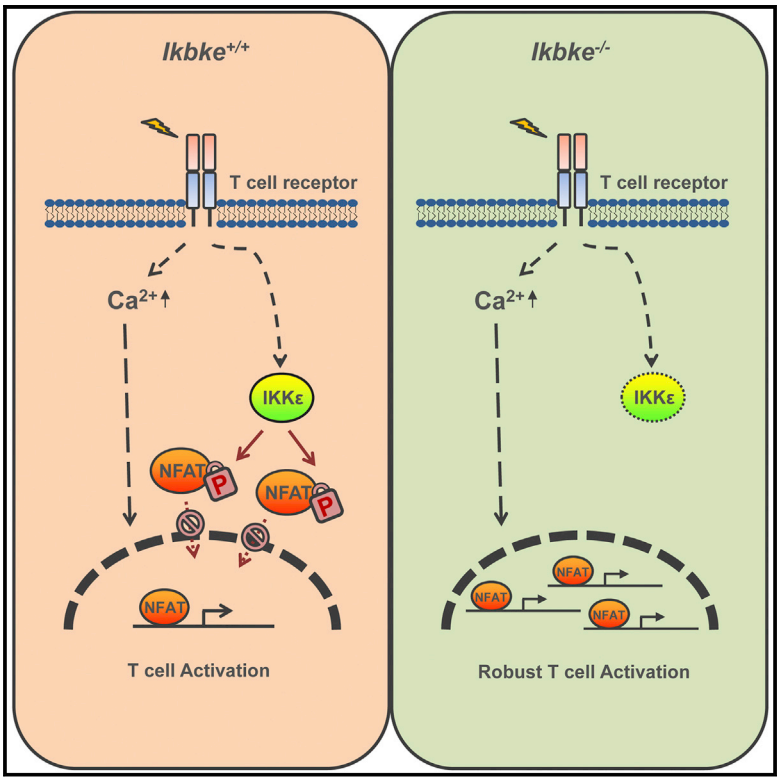

Authors

Junjie Zhang, Hao Feng, Jun Zhao, ..., Omid Akbari, Scott A. Tibbetts, Pinghui Feng

Correspondence

pinghui.feng@med.usc.edu

In Brief

Zhang et al. identify a negative feedback mechanism in which IKKε promotes NFATc1 phosphorylation to inhibit T cell responses. IKKε deficiency in mice leads to increased antiviral and antitumor T cell immunity and decreased persistent viral infection and tumor development.

Highlights

- IKKε is activated during T cell activation
- IKKε phosphorylates NFATc1 and inhibits NFAT activation
- Loss of IKKε elevates T cell responses against viral infection and tumor development
- IKKε is constitutively activated in tumor-bearing or persistently infected mice

Accession Numbers

GSE79074

Zhang et al., 2016, Cell Reports *16*, 405–418
July 12, 2016
http://dx.doi.org/10.1016/j.celrep.2016.05.083

Cell Reports
Article

IκB Kinase ε Is an NFATc1 Kinase that Inhibits T Cell Immune Response

Junjie Zhang,[1] Hao Feng,[1,2] Jun Zhao,[1] Emily R. Feldman,[3] Si-Yi Chen,[1] Weiming Yuan,[1] Canhua Huang,[4] Omid Akbari,[1] Scott A. Tibbetts,[3] and Pinghui Feng[1,*]

[1]Department of Molecular Microbiology and Immunology, Norris Comprehensive Cancer Center, University of Southern California, 1441 Eastlake Avenue, Los Angeles, CA 90033, USA

[2]Key Laboratory of Protein Chemistry and Developmental Biology of Education Ministry of China, College of Life Sciences, Hunan Normal University, Changsha, Hunan 410081, P.R. China

[3]Department of Molecular Genetics and Microbiology, College of Medicine, University of Florida, Gainesville, FL, 32610, USA

[4]State Key Laboratory of Biotherapy and Cancer Center, West China Hospital, and Collaborative Innovation Center for Biotherapy, Sichuan University, Chengdu, Sichuan 610041, P.R. China

*Correspondence: pinghui.feng@med.usc.edu

http://dx.doi.org/10.1016/j.celrep.2016.05.083

SUMMARY

Activation of nuclear factor of activated T cells (NFAT) is crucial for immune responses. IKKε is an IκB kinase (IKK)-related kinase, and the function of IKKε remains obscure in T cells, despite its abundant expression. We report that IKKε inhibits NFAT activation and T cell responses by promoting NFATc1 phosphorylation. During T cell activation, IKKε was transiently activated to phosphorylate NFATc1. Loss of IKKε elevated T cell antitumor and antiviral immunity and, therefore, reduced tumor development and persistent viral infection. IKKε was activated in CD8$^+$ T cells of mice bearing melanoma or persistently infected with a model herpesvirus. These results collectively show that IKKε promotes NFATc1 phosphorylation and inhibits T cell responses, identifying IKKε as a crucial negative regulator of T cell activation and a potential target for immunotherapy.

INTRODUCTION

Nuclear factors of activated T cells (NFATs) were originally identified as key regulators of T cell activation (Müller and Rao, 2010). The NFAT family consists of five transcription factors (NFATc1–NFATc4 and NFAT5) that share similar domain organization and structure. NFAT proteins contain an amino-terminal transactivation domain, a regulatory domain, a DNA-binding domain and a carboxyl-terminal domain that often harbors an additional transactivation domain (Chuvpilo et al., 1999, 2002; Müller and Rao, 2010). The regulatory domain contains multiple serine/threonine-rich motifs that can be phosphorylated by various kinases, e.g., casein kinase 1 (CK1), glycogen synthase kinase 3β (GSK3β), and the dual-specificity tyrosine-phosphorylation-regulated kinase (DYRK) (Müller and Rao, 2010). In resting cells, coordinated phosphorylation of NFAT by these kinases inactivates and excludes NFAT from the nucleus. Upon T cell activation, calcium influx activates numerous calcium-dependent enzymes, including the calcineurin phosphatase that dephosphorylates NFAT, which results in NFAT nuclear translocation and activation. NFAT is critical for not only the activation of T cells but also the function of other immune and non-immune cells (Greenblatt et al., 2010; Zanoni et al., 2009). In addition, NFAT plays essential roles in diverse fundamental biological processes, ranging from development to stem cell maintenance (Horsley et al., 2008; Müller et al., 2009). Derailed NFAT activation, not surprisingly, has been associated with tumor development and progression (Mancini and Toker, 2009). Therefore, identifying NFAT kinase is crucial for understanding the precise regulation of NFAT and the biological functions thereof.

IκB kinase (IKK) epsilon (IKKε), an inducible IKK-related kinase by inflammatory stimuli (Shimada et al., 1999), was originally discovered for its role in interferon production in response to viral infection (Fitzgerald et al., 2003; Sharma et al., 2003). Later, it was found to be dispensable for interferon production and primarily responsible for interferon-mediated antiviral activity via phosphorylating STAT (signal transducer and activator of transcription) transcription factors (Tenoever et al., 2007). Additionally, IKKε was identified as a breast cancer oncogene in a genome-wide screen and was later implicated in the development of other human cancers (Boehm et al., 2007; Guo et al., 2009). Much effort has been spent in identifying substrates of IKKε to understand its roles in cell transformation (Hutti et al., 2009; Shen et al., 2012; Xie et al., 2011). Notably, IKKε is abundantly expressed in T cells and is postulated to activate necrosis factor κB (NF-κB) downstream of T cell receptor (TCR) (Peters et al., 2000). Recent studies also indicate that IKKε is involved in interleukin (IL)-17-dependent signaling by phosphorylating the adaptor protein Act1 (Bulek et al., 2011) and contributes to the maintenance of Th17 cell through phosphorylating GSK3α (Gulen et al., 2012). Nevertheless, it is unclear how IKKε regulates T cell response in general, despite its abundant expression.

We report that IKKε promoted NFATc1 phosphorylation at multiple serine residues within the regulatory domain, which inhibited NFATc1 activation and T cell immune response. Mutation of these serine residues rendered NFATc1 resistance

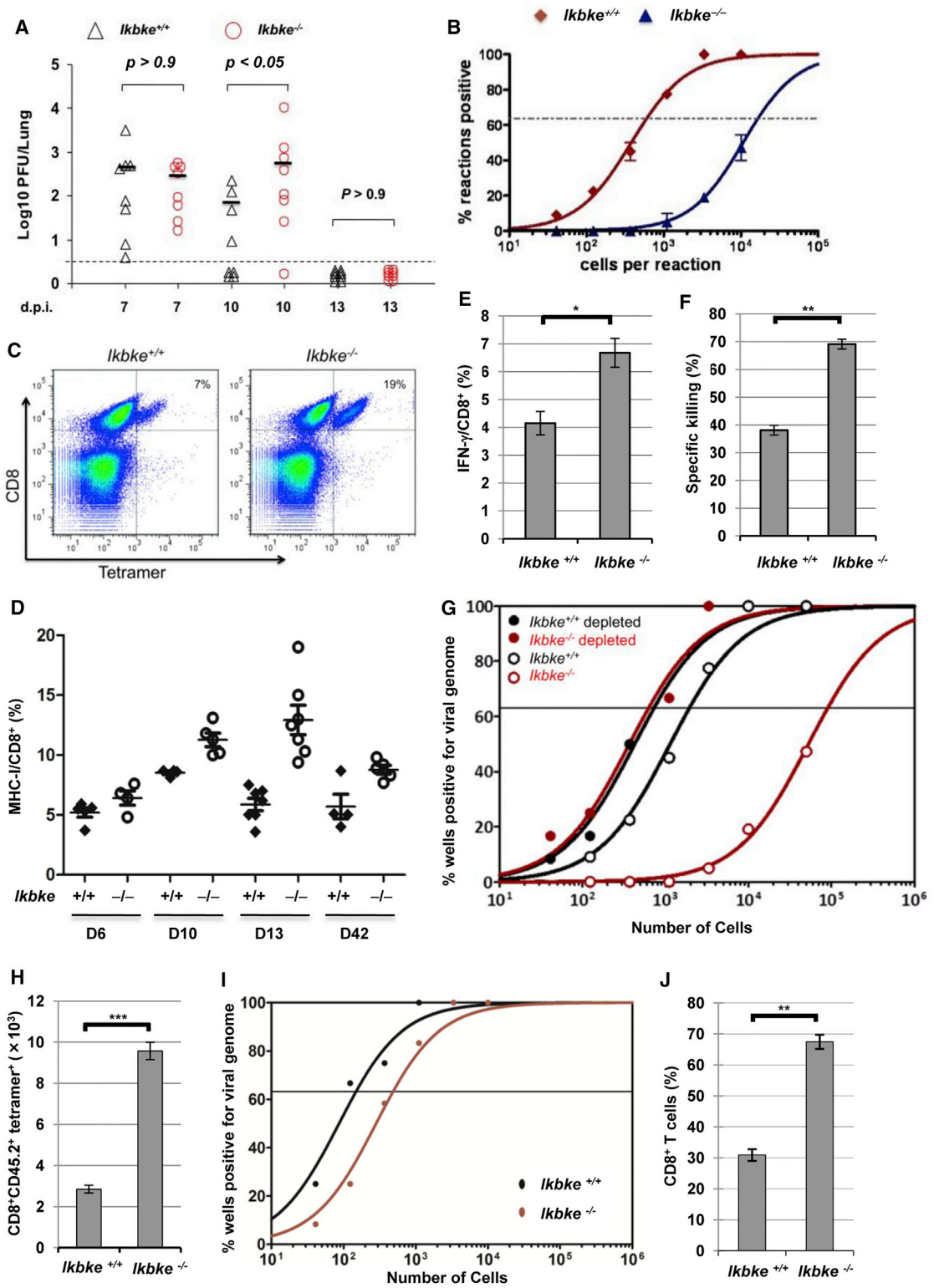

Figure 1. Loss of IKKε Reduces the Latent Infection of γHV68 and Boost Antiviral T Cell Immunity

Age- and gender-matched mice were infected with γHV68 via intranasal (A, 40 PFU) or intraperitoneal (B–J, 1 × 10^6 PFU) route.

(A) Viral lytic replication in the lung was determined by plaque assay at indicated days postinfection (dpi).

(B) Viral genome frequency at 42 dpi was determined by limiting-dilution PCR.

(legend continued on next page)

to IKKε-mediated phosphorylation and inhibition. Knockdown of IKKε elevated Jurkat T cell activation, while knockout of IKKε in mouse boosted T cell immunity and reduced persistent viral infection and tumor burden. Adoptive transfer and depletion experiments indicate that the elevated T cell immunity in IKKε-deficient mice resides in the $CD8^+$ T cell compartment. Our study reveals an unexpected function of IKKε, which acts as a critical negative regulator of T-cell-mediated immunity, possibly via phosphorylating NFAT transcription factors.

RESULTS

Loss of IKKε Reduces Herpesvirus Latent Infection

IKKε is implicated in regulating interferon response against RNA virus infection (Tenoever et al., 2007). To investigate the roles of IKKε in DNA virus infection, we infected wild-type (WT) and IKKε-deficient mice with murine gamma herpesvirus 68 (γHV68), a model herpesvirus closely related to human Kaposi's-sarcoma-associated herpesvirus (KSHV) and Epstein-Barr virus (EBV). Viral replications in the lung at 7 and 13 days post-infection (dpi) were similar (Figure 1A). At 10 dpi, the viral titer was higher in *Ikbke*$^{-/-}$ mice, suggesting the antiviral activity of IKKε against γHV68 at an early time point post-infection. A hallmark of herpesviruses is their propensity to establish latent infection. We further examined latent infection of γHV68 with limiting-dilution PCR. At 42 dpi, we detected a viral genome in 1 out of 200 splenocytes of WT mice (Figure 1B). Remarkably, loss of IKKε reduced viral genome frequency to 1 out of 10,000 splenocytes, a level equivalent to 2% of γHV68 latency in WT mice (Figure 1B). These results indicate that loss of IKKε greatly reduced viral latent infection.

Loss of IKKε Elevated the Antiviral Response of $CD8^+$ T Cells

A common denominator in immunity against persistent viruses is the T cell immune response. The dramatic reduction in γHV68 latent infection prompted us to delineate T cell response against γHV68. γHV68 infection in mice leads to a transient lytic replication phase lasting about 13 days, followed by the establishment of latent infection in lymphoid cells (e.g., B cells) (Doherty et al., 2001). When we infected mice with γHV68 via intraperitoneal injection, WT and *Ikbke*$^{-/-}$ mice had similar levels of splenomegaly (Figure S1A). The T cell counts in *Ikbke*$^{-/-}$ mice slightly increased compared to those of *Ikbke*$^{+/+}$ mice (Figure S1B). Loss of IKKε resulted in a 2- to 3-fold increase in virus-specific $CD8^+$ T cells at 13 dpi (Figure 1C). When $CD8^+$ T cell response was examined over time, we found that virus-specific $CD8^+$ T cells increased more rapidly in *Ikbke*$^{-/-}$ mice than in WT mice, from 6 to 10 dpi (Figure 1D). The difference peaked at 13 dpi, and the viral-specific $CD8^+$ T cell number in *Ikbke*$^{-/-}$ mice was 3-fold that in WT mice (Figure S1C). More *Ikbke*$^{-/-}$ $CD8^+$ T cells produced interferon (IFN)-γ compared to WT cells when stimulated with viral peptide (Figure 1E). Spleen viral load (genome copy number) was comparable in WT and *Ikbke*$^{-/-}$ mice at 6 and 10 dpi, but the viral load in *Ikbke*$^{-/-}$ mice was 50% of that in WT mice at 13 dpi (Figure S1D). Although the overall spleen structure was similar between mock- and γHV68-infected mice, germinal centers were expanded in the virus-infected spleens of WT and *Ikbke*$^{-/-}$ mice compared to mock-infected spleens (Figure S1E). γHV68 infection in WT and *Ikbke*$^{-/-}$ mice induced equivalent amounts of virus-specific antibodies in sera (Figure S1F) and comparable levels of IL-6 and CCL5 in spleen (Figure S1G). These results agree with previous reports that IKKε is dispensable for cytokine production in response to viral infection (Tenoever et al., 2007).

Next, we performed an in vivo killing assay to assess the functionality of the increased $CD8^+$ T cells in γHV68-infected mice. We observed a 40% reduction of antigen-loaded target cells in γHV68-infected WT mice. Remarkably, antigen-bearing splenocytes decreased by 70% in γHV68-infected *Ikbke*$^{-/-}$ mice, indicative of an increased cytotoxic lysis by $CD8^+$ T cells (Figures 1F and S1H). To determine the effectiveness of $CD8^+$ T cells in reducing γHV68 latent infection, we depleted $CD8^+$ T cells with specific antibody from 16 dpi (Figure S2A). The depletion slightly increased viral genome frequency in the splenocytes of WT mice, which is consistent with the role of $CD8^+$ T cells in controlling viral latent infection (Cardin et al., 1996). Remarkably, depletion of $CD8^+$ T cells in IKKε-deficient mice completely restored the viral latent infection level to that of WT mice treated with anti-CD8 antibody (Figure 1G). The curves of γHV68 latent infection were identical in WT and IKKε-deficient mice that were depleted of $CD8^+$ T cells, indicating that the elevated $CD8^+$ T cell response in IKKε-deficient mice is primarily responsible for the deficit of γHV68 latent infection. These results collectively support the conclusion that loss of IKKε increases $CD8^+$ T cell response, which, in turn, diminishes γHV68 latent infection.

To test whether IKKε has an intrinsic activity in $CD8^+$ T cells, we transferred equal numbers of WT or IKKε-deficient (CD45.2) $CD8^+$ T cells into immune-competent CD45.1 recipient mice,

(C) Representative tetramer staining (ORF61) at 13 dpi.
(D) Tetramer staining was performed at indicated dpi.
(E) Splenocytes were isolated from γHV68-infected *Ikbke*$^{+/+}$ and *Ikbke*$^{-/-}$ mice at 13 dpi and stimulated with viral antigenic peptide (ORF61). IFN-γ was determined by intracellular staining.
(F) Splenocytes labeled with CFSE were pulsed with or without viral peptide and transferred into γHV68 infected *Ikbke*$^{+/+}$ and *Ikbke*$^{-/-}$ mice. The specific killing was quantified.
(G) *Ikbke*$^{+/+}$ and *Ikbke*$^{-/-}$ mice were mock treated or depleted with anti-CD8 antibody starting at 16 dpi. Splenocytes were harvested at 42 dpi, and viral genome frequency was determined as in (B).
(H and I) $CD8^+$ splenocytes of *Ikbke*$^{+/+}$ or *Ikbke*$^{-/-}$ mice were transplanted into CD45.1 immune-competent mice infected with γHV68 for 16 days. $CD8^+$ T cell response and viral latent infection in the splenocytes were analyzed by tetramer staining (H) and limiting-dilution PCR (I), respectively.
(J) *Ikbke*$^{+/+}$ and *Ikbke*$^{-/-}$ $CD8^+$ splenocytes were mixed and transferred into *Rag-2*$^{-/-}$ mice that were infected with γHV68. At 13 dpi, splenocytes were harvested and analyzed for CD45.1 (*Ikbke*$^{+/+}$) and CD45.2 (*Ikbke*$^{-/-}$) within the $CD8^+$ T cell subset.
Error bars denote SD. *$p < 0.05$; **$p < 0.01$; ***$p < 0.001$.

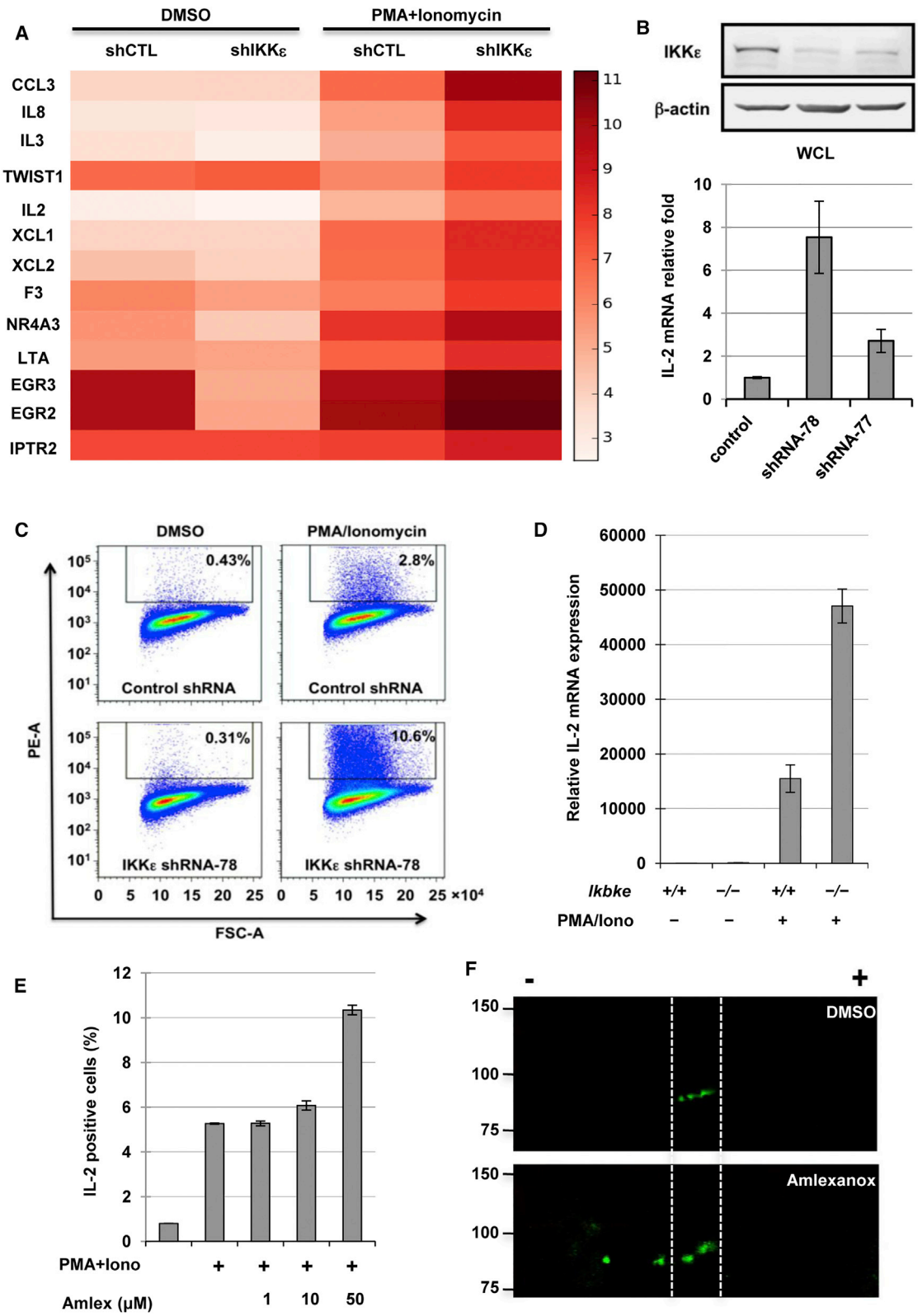

Figure 2. Knockdown or Pharmacological Inhibition of IKKε Promotes T Cell Activation

(A) Jurkat T cells transduced with control shRNA (shCTL) or shRNA against IKKε (shIKKε) were treated with DMSO or PMA plus ionomycin for 3 hr. Total RNA was extracted and analyzed by microarray. Top differentially expressed genes were shown. Color intensity denotes $\log_2$ normalized raw data.

(legend continued on next page)

and the mice were then infected with γHV68. We observed that the virus-specific $CD8^+$ T cell population in *Ikbke*$^{-/-}$ mice was approximately 3-fold that in *Ikbke*$^{+/+}$ mice at 16 dpi (Figures 1H and S2B). Moreover, γHV68 latent infection in mice that received *Ikbke*$^{-/-}$ $CD8^+$ T cells was reduced by 60%–70%, compared to that in mice that received *Ikbke*$^{+/+}$ $CD8^+$ T cells (Figure 1I). We also transferred WT and *Ikbke*$^{-/-}$ $CD8^+$ T cells into *Rag-2*$^{-/-}$ mice and examined T cell expansion after γHV68 infection. There were two times as many *Ikbke*$^{-/-}$ $CD8^+$ T cells as WT $CD8^+$ T cells at 13 dpi (Figures 1J and S2C). These results demonstrate an intrinsic role of IKKε in $CD8^+$ T cell activation and expansion.

Knockdown of IKKε Elevates T Cell Response

To explore how IKKε inhibits T cell activation, we analyzed the gene expression profile of Jurkat T cells in which IKKε was depleted with short hairpin RNA (shRNA). Treatment with PMA and ionomycin upregulated the expression of a few hundred genes in WT cells (GEO: GSE79074), among which the expression of ~50 genes was further increased in IKKε-depleted cells upon activation (Figure 2A). This notable class of genes that were significantly upregulated by IKKε knockdown is composed of chemokines and chemotaxis-associated factors that are regulated by NFAT activation, including CCL3, IL-2, IL-8, XCL1, and XCL2. This result suggests that IKKε may regulate NFAT transcription factors in T cells.

Next, we examined the mRNA and protein expression of IL-2 as surrogates to monitor NFAT activation regulated by IKKε. Two IKKε shRNAs increased IL-2 mRNA by factors of 7 and 3 (Figure 2B) and the percentage of IL-2-positive cells by 2- to 4-fold (Figures 2C, S3A, and S3B) in stimulated Jurkat T cells. While the expression of WT IKKε had no detectable effect on IL-2 mRNA and protein levels, the expression of the kinase-deficient mutant IKKεK38A elevated IL-2 mRNA and protein by factors of 3.5 and 2, respectively (Figures S3C–S3E). These results suggest that IKKεK38A has a dominant-negative effect on endogenous IKKε to elevate NFAT activation. The lack of inhibition of IL-2 gene expression by exogenous IKKε suggests that endogenous IKKε is sufficient to suppress NFAT activation. Moreover, IL-2 mRNA of mouse primary *Ikbke*$^{-/-}$ T cells was 3-fold that of WT T cells upon stimulation (Figure 2D). Given that TBK-1 is closely related to IKKε, we knocked down TBK-1 in Jurkat T cells, with or without IKKε knockdown, and found that TBK-1 knockdown had no significant effect on IL-2 expression (Figures S3F–S3I). These results suggest that TBK-1 is dispensable in regulating NFAT upon T cell activation. A recent study has identified amlexanox, a drug clinically prescribed to treat oral ulcers, as a specific inhibitor of IKKε (Reilly et al., 2013). Consistent with this, treatment with amlexanox increased the percentage of IL-2-positive T cells in a dose-dependent manner (Figure 2E). IL-2 expression in Jurkat T cells is highly dependent on NFAT dephosphorylation and activation (Chow et al., 1999). Thus, we examined the effect of amlexanox on the dephosphorylation of NFATc1. Two-dimensional gel electrophoresis analysis demonstrated that, when IKKε was inhibited with amlexanox, NFATc1 shifted toward the negatively charged side in the first dimension and migrated faster in the second dimension (Figure 2F), indicating reduced phosphorylation that was recapitulated by treatment with alkaline phosphatase (Figure S3J). Thus, amlexanox treatment inhibits IKKε and reduces NFATc1 phosphorylation, which may lead to increased T cell activation. Collectively, these results indicate that IKKε is a key negative regulator of NFAT activation and T cell response.

IKKε Inhibits NFAT Activation

Our previous studies showed that a viral G-protein-coupled receptor (vGPCR) can potently activate NFAT (Zhang et al., 2015) (Figure S4A). Next, we used an NFAT reporter assay to examine the effect of IKKε on vGPCR-induced NFAT activation. IKKε expression reduced NFAT activation by vGPCR in a dose-dependent manner (Figure S4B). To probe the point of inhibition by IKKε, we overexpressed NFATc1 and calcineurin (CnA) to activate NFAT. Strikingly, the expression of IKKε was sufficient to diminish NFAT activation induced by both molecules (Figures S4C and S4D). Moreover, IKKε was as potent as DYRK2 in diminishing NFAT activation induced by NFATc1 (Figure 3A). IKKα and IKKβ, however, only weakly inhibited CnA-induced NFAT activation (Figures S4E and S4F), further prompting us to focus on IKKε for its regulatory roles in NFAT activation. To test whether the kinase activity of IKKε is required for its inhibition of NFAT activation, we examined the effect of IKKεK38A on NFAT activation. IKKε, but not IKKεK38A, abolished CnA-induced NFAT activation in a dose-dependent manner (Figure 3B). Similarly, IKKε abrogated the nuclear translocation of EGFP-NFATc1 upon treatment with ionomycin, whereas IKKεK38A had no detectable effect on NFATc1 nuclear translocation (Figures 3C and 3D). Collectively, these results indicate that IKKε potently inhibits NFAT activation in a kinase-dependent manner.

IKKε Promotes NFATc1 Phosphorylation via Direct and Indirect Mechanisms

Since NFAT activation is primarily enabled by dephosphorylation (Müller and Rao, 2010), and the kinase activity of IKKε is required for its inhibition of NFAT activation, we reasoned that IKKε likely phosphorylates NFAT. Expression of NFAT kinases often retards NFAT migration as analyzed by electrophoresis. Indeed, exogenously expressed IKKε resulted in a more slowly migrating species of NFATc1 (Figure 4A). The expression of IKKα, IKKβ, or IKKεK38A failed to retard NFATc1 migration (Figures 4A and S5A). Furthermore, purified IKKε, but not IKKεK38A, was able

(B and C) Jurkat T cells were transduced with lentiviral shRNA and whole-cell lysates were analyzed by immunoblotting (B, top) and total RNA was analyzed by reverse transcription qPCR (B, bottom). IL-2 protein expression was examined by intracellular staining (C).
(D) Isolated mouse $CD3^+$ primary T cells were stimulated with PMA and ionomycin and IL-2 mRNA level was analyzed by real-time q-PCR.
(E) Jurkat T cells were stimulated with PMA and ionomycin (Iono), with increasing concentrations of amlexanox (Amlex) and analyzed by IL-2 intracellular staining.
(F) Jurkat T cells stably expressing NFATc1 were activated with PMA plus ionomycin without (DMSO) or with amlexanox (50 μM). Precipitated NFATc1 was analyzed by two-dimensional gel electrophoresis and immunoblotting.
Error bars denote SD.

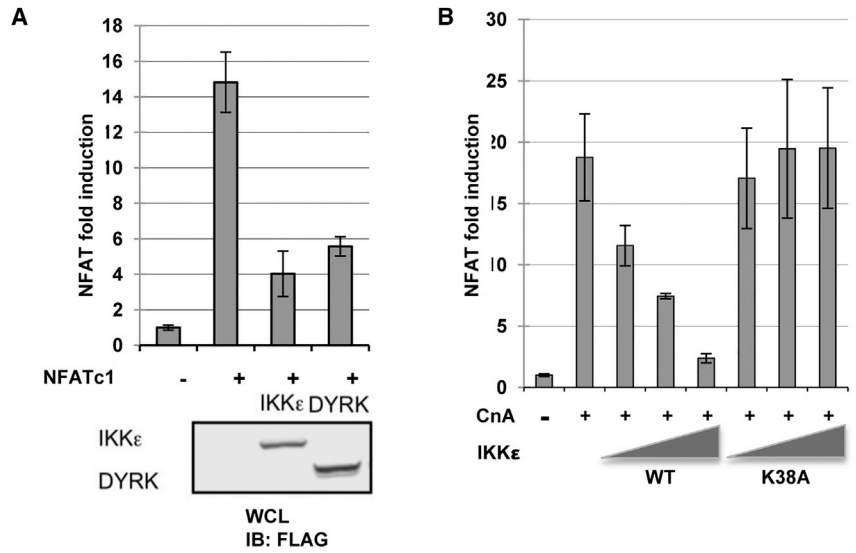

Figure 3. IKKε Inhibits NFAT Activation in a Kinase-Dependent Manner

(A) 293T cells were transfected with a NFAT reporter plasmid cocktail and plasmids containing the indicated genes. NFAT activation was determined by luciferase assay. WCL, whole-cell lysate; IB, immunoblotting.

(B) Reporter assay was performed as in (A), except that increasing amounts of plasmid containing WT IKKε or IKKεK38A were used.

(C and D) 293T cells were transfected with EGFP-NFATc1 alone or together with IKKε or IKKεK38A. Cells were treated with ionomycin (1 μM) for 1 hr. NFATc1 subcellular localization was analyzed by fluorescence microscopy. Representative images were shown (C). Around 300 cells were counted for nuclear NFATc1 localization, and percentage was calculated (D).

Error bars denote SD.

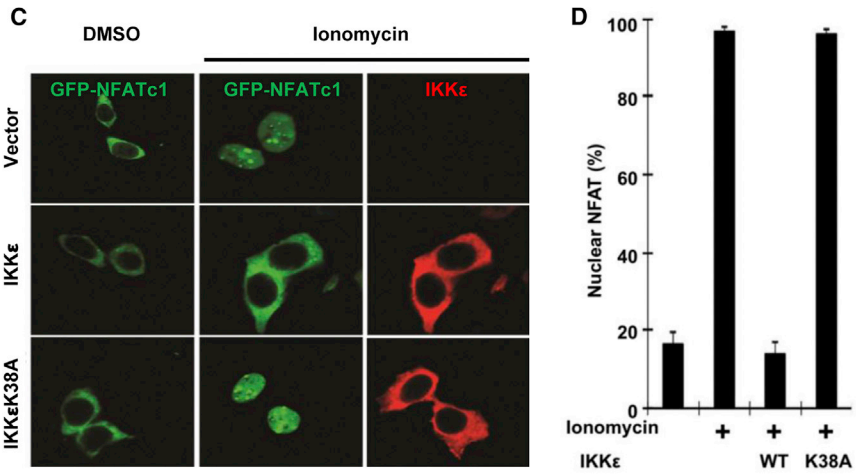

to phosphorylate the N-terminal regulatory domain (amino acids [aa] 1–319) of NFATc1 in vitro (Figure 4B). Screening glutathione S-transferase (GST) fusion proteins carrying known phosphorylation motifs, we found that IKKε efficiently phosphorylated the SP3 motif and weakly phosphorylated the SP2 sequence but not SP1, SRR1, SRR2, or KTS sequences (Figure S5B). Further mutational analysis of SP2 and SP3 sequences identified two serine residues, not those classical SP sequences, which served as phospho-acceptors (Figure S5C). These two serine residues are embedded in a conserved motif, SVTDD(/EE)SWLG (Figure S5D). An in vitro kinase assay indicated that the second serine residue was the primary phosphorylation site (Figure S5D). Given the close proximity of these IKKε phosphorylation sites to the SP sequences, we tested whether IKKε can prime the SP sites for GSK3β-mediated phosphorylation. Pre-phosphorylation of SP2 and SP3 by PKA led to robust phosphorylation by GSK3β, while IKKε failed to do so, indicating that IKKε cannot prime NFAT for GSK3β-mediated phosphorylation of SP sites (Figure S5E).

To delineate the IKKε phosphorylation sites within NFATc1, we purified NFATc1 from 293T cells with or without IKKε expression and analyzed serine/threonine phosphorylation by mass spectrometry. We identified four principal phosphorylation sites, in addition to the two serine residues in the SP3 site, within the N-terminal regulatory domain (Figure 4C). S^{117} of the CnA-docking site and two residues in the SP3 sequences are relatively conserved among NFAT proteins (Figure S5F). Phosphorylation frequency of three sites (S^{117}, S^{151}, and S^{324}) was approximately doubled by IKKε expression, whereas that of S^{161} was increased from the basal level of 13% to 76% with IKKε expression. S^{117} of the CnA-docking site was shown to be phosphorylated by the Jun N-terminal kinase (JNK), which reduced the CnA-binding ability of NFATc1 (Chow et al., 1997). Using an antibody specific for the phosphorylated S^{117}PRIEIT epitope, we found that exogenous IKKε expression greatly elevated the phosphorylation of the CnA-docking site (Figure 4D). Next, we tested whether IKKε can directly phosphorylate these motifs in vitro. Except for the peptide containing S^{117}, the other peptides can be phosphorylated by IKKε in vitro (Figures S5G and S5H). However, IKKε expression greatly increased the phosphorylation of the CnA-docking peptide (S^{117}) in transfected cells (Figure S5I). These findings suggest that other kinases, such as the aforementioned JNK (Chow et al., 1997), may relay signal transduction from IKKε to NFAT by directly phosphorylating the CnA-docking site. We also confirmed that the phosphorylation-mimetic mutation (S > E) of the CnA-docking site diminished CnA binding by in vitro GST pull-down (Figure S5J). These results collectively demonstrate that IKKε promotes NFATc1 phosphorylation via direct and indirect mechanisms.

To probe the functional consequence of these phosphorylation sites, we generated NFATc1 mutants carrying S > A mutations. Reporter assays showed that a single S > A mutation of four serines (S^{117}, S^{151}, S^{161}, S^{324}) within the N-terminal region

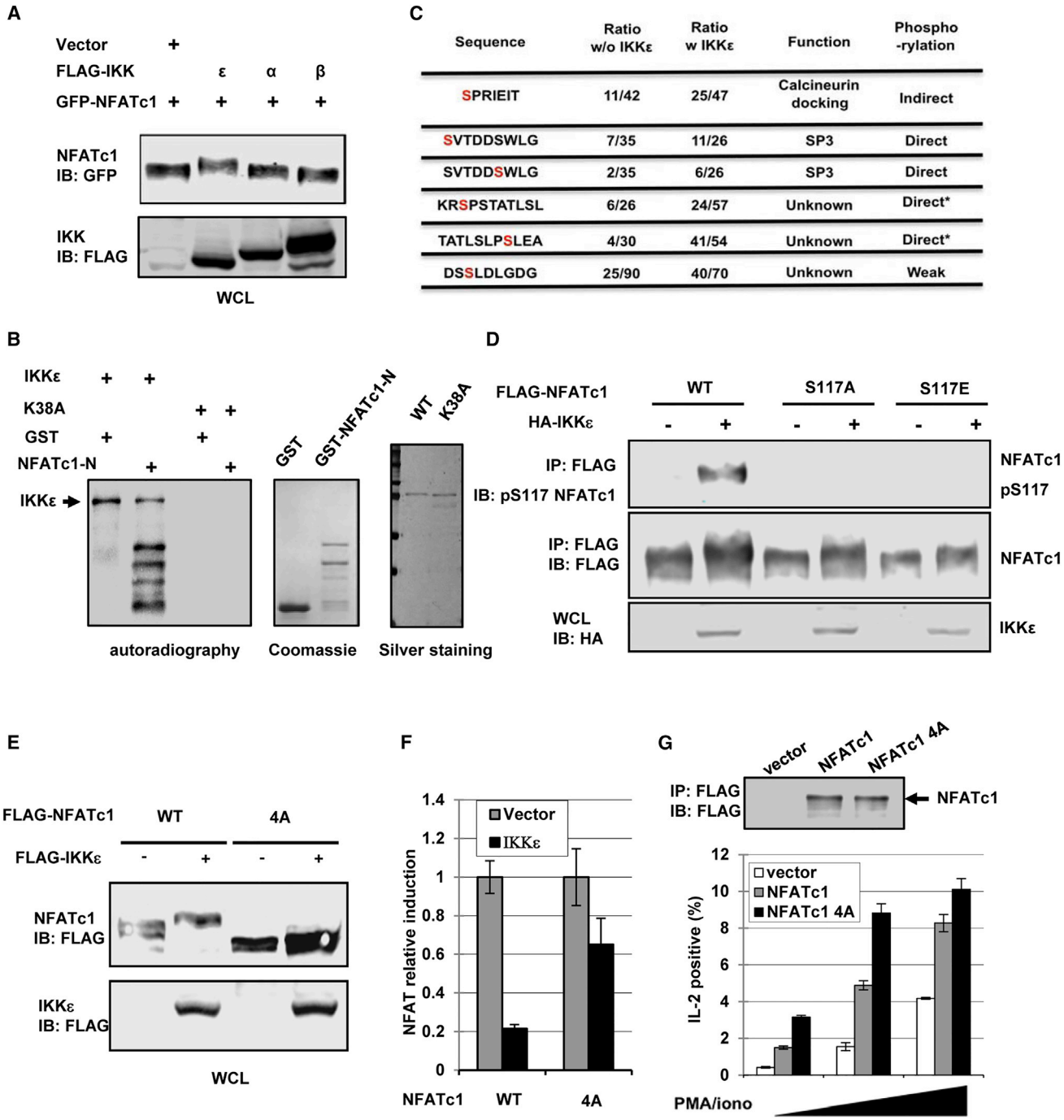

Figure 4. IKKε Phosphorylates NFATc1

(A) 293T cells were transfected with plasmids containing EGFP-NFATc1 and the indicated IKK. Whole-cell lysates (WCL) were analyzed by immunoblotting (IB) with the indicated antibodies.

(B) In vitro kinase assay was performed using purified GST fusion proteins containing the N-terminal regulatory domain (1–319) of NFATc1. IKKε and IKKεK38A were purified from 293T cells (silver staining), while GST and GST-NFATc1-N were purified from bacteria.

(C) Summary of the IKKε phosphorylation sites.

(D) 293T cells were transfected with plasmids containing the indicated genes. NFATc1 was precipitated with anti-FLAG antibody and, along with whole-cell lysates (WCL), analyzed by immunoblotting.

(E) 293T cells were transfected with plasmids containing the indicated genes, and whole-cell lysates were analyzed by immunoblotting.

(legend continued on next page)

conferred partial resistance to IKKε-mediated inhibition (Figure S5K). Mutations in the SP3 sequence had no apparent effect on NFATc1-dependent gene expression (data not shown), suggesting that these phosphorylations are involved in functions other than transcription regulation of NFATc1. Alternatively, these phosphorylations may be redundant with other phosphorylations in regulating NFATc1-dependent gene expression. Thus, we focused on the other four serines (S^{117}, S^{151}, S^{161}, and S^{324}) for this study. When all four S > A mutations were introduced into NFATc1, this mutant (designated NFATc1-4A) was refractory to IKKε-mediated phosphorylation and inhibition (Figures 4E and 4F). By contrast, DYRK2 expression retarded the migration of NFATc1-4A and WT NFATc1 to a similar degree (Figure S5L). We noted that IKKε expression slightly retarded the migration of NFATc1-4A, implying that other minor IKKε phosphorylation sites exist in NFATc1. These results identified major phosphorylation sites within the N-terminal regulatory domain specifically impacted by IKKε. Next, we expressed NFATc1-4A and WT NFATc1 in Jurkat T cells and determined IL-2 protein expression. NFATc1-4A expression doubled the percentage of IL-2-positive cells compared to WT NFATc1 upon stimulation, while NFATc1 and NFATc1-4A were equally expressed in Jurkat cells (Figure 4G). Collectively, IKKε inhibits NFAT activation through increasing NFATc1 phosphorylation.

IKKε Kinase Activity Is Coupled to T Cell Activation

The inhibition of NFAT by IKKε may provide negative feedback to T cell activation. We examined whether IKKε and NFATc1 co-elute in lysates of resting and activated Jurkat T cells by gel filtration. In resting T cells, NFATc1 was primarily eluted in fractions corresponding to protein sizes of 440–670 kDa, whereas IKKε was widely distributed in fractions corresponding to protein sizes of 120–670 kDa, which demonstrated partly overlapped co-elution (Figure 5A). NFATc1 was highly induced in activated T cells and primarily co-eluted with IKKε in fractions corresponding to protein sizes of 150–670 kDa. By contrast, IKKβ demonstrated a broader elution, with peak elution in fractions corresponding to sizes >670 kDa in resting and activated Jurkat T cells. Next, we monitored the activation of IKKε with an antibody specific for phosphorylated serine 172, a marker for activated IKKε, upon T cell activation. When T cells were stimulated with antibodies against CD3 and CD28, IKKε activation was detected as early as 10 min and lasted 30 min after stimulation (Figure 5B). Similar kinetics of IKKε phosphorylation was also observed when T cells were activated by PMA and ionomycin. Despite the finding that knockdown of TBK-1 has no impact on NFAT activation, we found that T cell activation by antibodies against CD3 and CD28 also activated TBK-1 (Figure S6A). These results indicate that T cell activation upregulates the kinase activity of IKKε.

Six NFATc1 isoforms are generated in lymphocytes, and they form three major bands in immunoblot analysis (Muhammad et al., 2014; Rudolf et al., 2014; Serfling et al., 2006). Upon T cell activation, NFATc1 was quickly dephosphorylated and then phosphorylated at around 60 min. In contrast, NFATc1 was still partly dephosphorylated in IKKε-depleted cells at 120 min post-stimulation (Figure 5C). Thus, IKKε contributes to NFATc1 phosphorylation and potentially restricts its rapid activation during T cell activation. Next, we developed an antibody that specifically reacted with a peptide carrying the phosphorylated serine 161 of NFATc1 (Figure S6B). NFATc1 phosphorylation was detected at 10–30 min post-stimulation, while NFATc1 phosphorylation was abolished in Jurkat T cells in which IKKε was silenced (Figure 5C). To determine whether IKKε translocates into the nucleus where NFAT export kinases exert their function, we performed fractionation to obtain cytosolic and nuclear extract. Interestingly, IKKε remained in the cytosolic fraction even when T cells were activated (Figure S6C). IKKε was implicated in enabling the activation of STAT and NF-κB transcription factors via direct phosphorylation (Peters et al., 2000; Tenoever et al., 2007). Thus, we determined the expression of two classic NF-κB-dependent genes, A20 (*TNFAIP1*) and IκBα (*NFKBIA*), in Jurkat T cells when IKKε was silenced. We found that knockdown of IKKε had no apparent effect on the expression of A20 and IκBα (Figure S6D). Furthermore, T cell activation did not induce STAT1 phosphorylation as IFN-β treatment did (Figure S6E). These results show that IKKε depletion does not impact NF-κB activation at early time points and that STAT1 is not phosphorylated at T708 in activated T cells.

To simultaneously probe the phosphorylation of multiple sites in NFATc1 by IKKε during T cell activation, we established a Jurkat T cell line stably expressing FLAG-NFATc1 and quantitatively analyzed purified NFATc1 with mass spectrometry for phosphorylation. In resting T cells, the phosphorylated S^{161} can be detected at a low level, whereas phosphorylation of the other three sites was below detection (Figure 5D). In activated T cells, the phosphorylation of S^{117}, S^{151}, S^{161}, and S^{324} increased significantly (Figure 5D). When IKKε was inhibited with amlexanox in activated T cells, the phosphorylation of all four sites decreased to the level below detection (Figure 5D). This result demonstrates the critical roles of IKKε in promoting the phosphorylation of all four sites within NFATc1. Upon T cell activation, NFAT translocates into the nucleus and binds to NFAT regulatory elements (promoters and enhancers) to initiate gene transcription. Importantly, the nuclear translocation of NFATc1 and NFATc2 was significantly increased in activated T cells with IKKε knockdown (Figure 5E). Furthermore, a chromatin immunoprecipitation (ChIP) assay demonstrated higher binding of NFATc1 and NFATc2 to the IL-2 promoter in IKKε knockdown T cells or IKKε-deficient $CD8^+$ T cells upon activation (Figures 5F and S6F). Using purified mouse $CD8^+$ T cells, we showed that the kinase activity of IKKε was increased in activated mouse T cells, and NFATc1 was phosphorylated by IKKε (Figure 5G). These results show that IKKε restricts NFAT nuclear translocation during T cell

(F) NFAT activation in 293T cells by NFATc1-4A mutant was determined by luciferase assay.
(G) Jurkat T cells were infected with control lentivirus or lentivirus containing WT NFATc1 or NFATc1-4A mutant. NFATc1 was precipitated and analyzed by immunoblotting (top). After stimulation, the cells were analyzed by IL-2 intracellular staining (bottom).
Error bars denote SD.

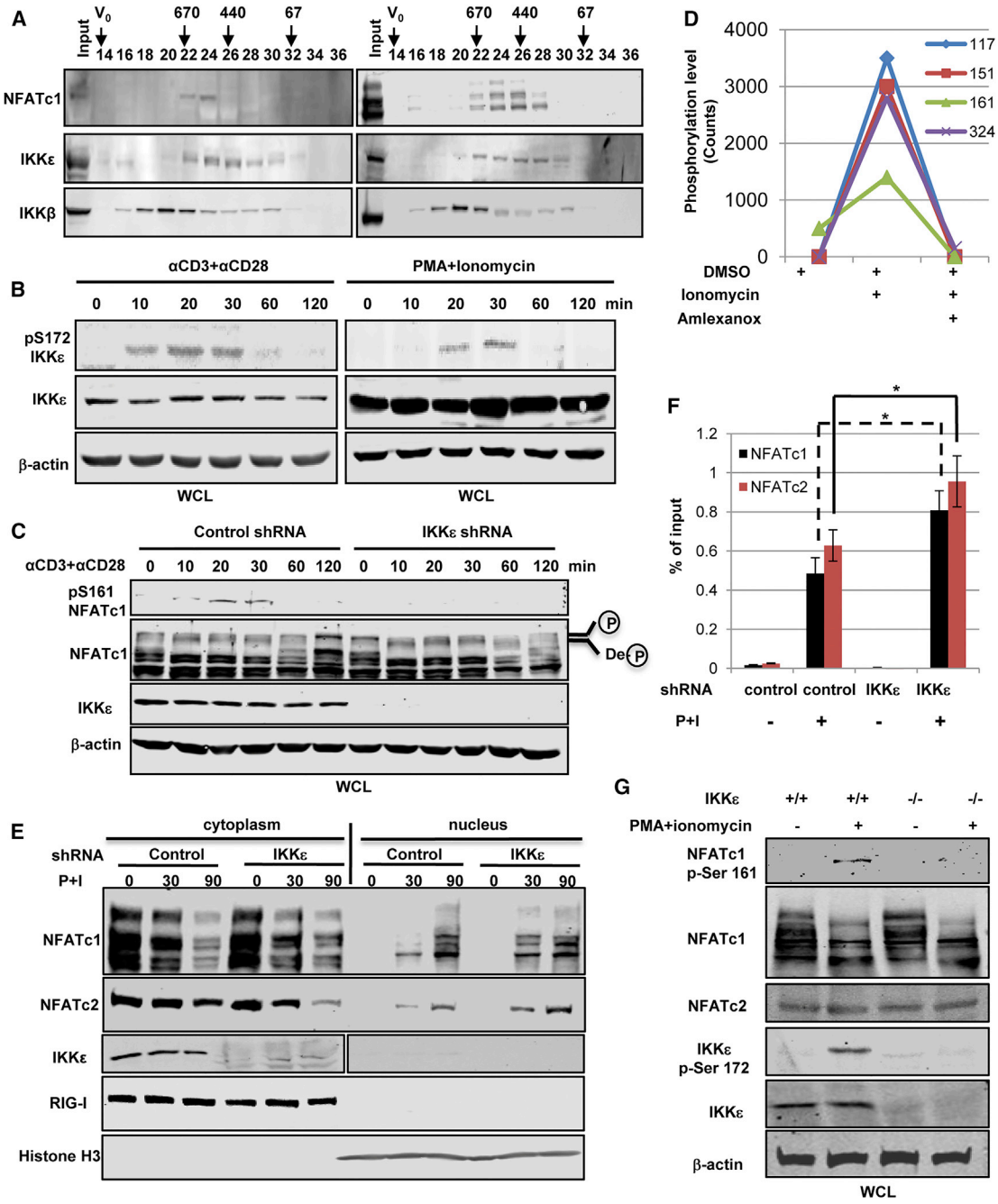

Figure 5. T Cell Activation Upregulates the Kinase Activity of IKKε

(A) Jurkat T cells were mock treated or stimulated with PMA plus ionomycin for 1 hr. Cell extracts were analyzed by gel filtration chromatography with superose 6. Fractions were analyzed by immunoblotting with indicated antibodies. V_0, void volume. Numbers at the top indicate the size of protein complex in kilodaltons.

(B) Jurkat T cells were treated with antibodies against CD3 and CD28 (left panels) or PMA plus ionomycin. WCLs were analyzed by immunoblotting. WCL, whole-cell lysate.

(C) Jurkat T cells expressing control shRNA or IKKε-shRNA were stimulated and analyzed by immunoblotting. P, phosphorylation.

(D) Jurkat T cells stably expressing FLAG-NFATc1 were stimulated with vehicle (DMSO) or ionomycin, with or without Amlexanox (50 μM) for 2 hr. NFATc1 was affinity purified and analyzed by mass spectrometry for quantitative measurement of phosphorylation of peptides containing S^{117}, S^{151}, S^{161}, and S^{324}.

(E) Jurkat T cells were stimulated and fractionated into the cytoplasmic and nuclear fractions for immunoblotting analysis. P+I, PMA plus ionomycin.

(F) Jukat T cells were stimulated for 1 hr, and chromatin immunoprecipitation (ChIP) was performed using NFATc1 or NFATc2 antibodies. The enrichment of IL-2 promoter was determined by qPCR.

(G) Purified mouse $CD8^+$ T cells were stimulated with PMA and ionomycin, and WCLs were analyzed by immunoblotting.

Error bars denote SD. *$p < 0.05$.

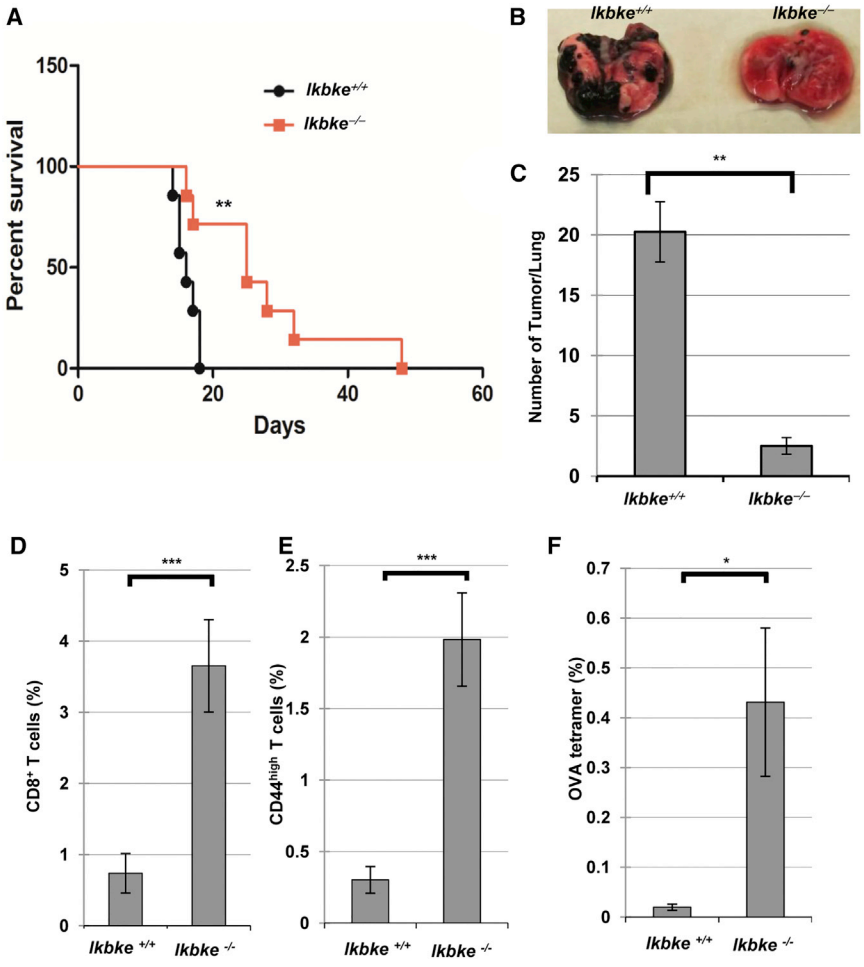

Figure 6. Loss of IKKε Elevates T Cell Antitumor Immunity and Reduces Tumor Development

(A) Gender- and age (9- to 10-month-old)-matched *Ikbke*$^{+/+}$ and *Ikbke*$^{-/-}$ mice were inoculated with B16 MO5 cells via tail-vein injection. Mouse survival was showed by Kaplan-Meyer survival curves.

(B–F) Gender- and age (10- to 12-week-old)-matched *Ikbke*$^{+/+}$ and *Ikbke*$^{-/-}$ mice were inoculated with B16 MO5 cells via tail-vein injection. Mice were euthanized at 32 days after inoculation. Representative lungs were photographed (B) and tumors were enumerated (C). The isolated lung cells were analyzed by staining of CD8 (D), CD44 (E), and OVA tetramer (F).

Error bars denote SD. *p < 0.05; **p < 0.01; ***p < 0.001.

activation. Taken together, T cell activation upregulates the kinase activity of IKKε, which, in turn, phosphorylates NFAT, providing a possible negative feedback to curtail T cell activation.

Loss of IKKε Elevates T Cell Antitumor Immunity and Reduces Tumor Development

Viral persistent infection is a physiological condition relevant to the chronic development of cancers. The elevated CD8$^+$ immunity in *Ikbke*$^{-/-}$ mice greatly reduced persistent viral infection, and the elevated CD8$^+$ T cell response can be beneficial in tumor control. Thus, we determined whether IKKε-deficient mice are more resistant to tumor development than WT mice, using the B16 melanoma mouse model. While WT mice succumbed to a lethal dose of B16 melanoma cells in an average of 16 days, the IKKε-deficient mice survived for an average of 29 days after inoculation of melanoma cells (Figure 6A). IKKε-deficient mice harbored one-eighth as many tumors as WT mice (Figures 6B and 6C). These results collectively show that loss of IKKε renders mice more resistant to metastatic melanoma development.

We determined CD8$^+$ T cell immune response to MO5 melanoma cell, a B16-derived cell line that expresses the well-defined ovalbumin epitope SIINFEKL, which readily enables the quantification of antitumor T cell immune response. We found that lungs of IKKε-deficient mice harbored 4-fold as many CD8$^+$ T cells as those of WT mice (Figure 6D). A high level of CD44 expression serves as a marker for activated antitumor T cells (Okoye et al., 2015). There were 0.3% and 2% of CD44^{high} T cells in the lungs of WT and IKKε-deficient mice, respectively (Figure 6E). Moreover, loss of IKKε also increased OVA-specific CD8$^+$ T cells in the lung by more than 10-fold (Figure 6F). The percentage of the CD44^{high} population of CD8$^+$ T cells, however, only marginally increased in IKKε-deficient mice, compared to WT mice (Figure S7A). The PD-1 expression on CD8$^+$ T cells was also marginally decreased in IKKε-deficient mice (Figure S7B). These results collectively support the finding that loss of IKKε results in elevated numbers of activated CD8$^+$ T cells in the tumor microenvironment.

IKKε in CD8$^+$ T Cells Is Activated in Mice Persistently Infected with γHV68 or Bearing Chronic Tumor

Depletion of CD8$^+$ T cells increased viral latent infection by less than 2-fold in WT mice but more than 100-fold in IKKε-deficient mice (Figure 1G). This result suggests that viral persistent infection activates IKKε to suppress the antiviral immune response of CD8$^+$ T cells. To test this hypothesis, we isolated T cells from mice latently infected with γHV68 and examined IKKε activation and NFAT phosphorylation. Immunoblotting analysis showed an increased NFATc1 phosphorylation (S^{161}) in CD8$^+$ T cells of γHV68-infected mice, compared to those of mock-infected mice (Figure 7A). Semiquantitative densitometry analysis indicated that, in comparison to mock-infected mice, there was a 4-fold increase of phosphorylated NFATc1 in γHV68-infected mice (Figure 7B). Consistent with this, we observed a slight increase in IKKε protein expression and a significant increase in S^{172}-phosphorylated IKKε (Figures 7A

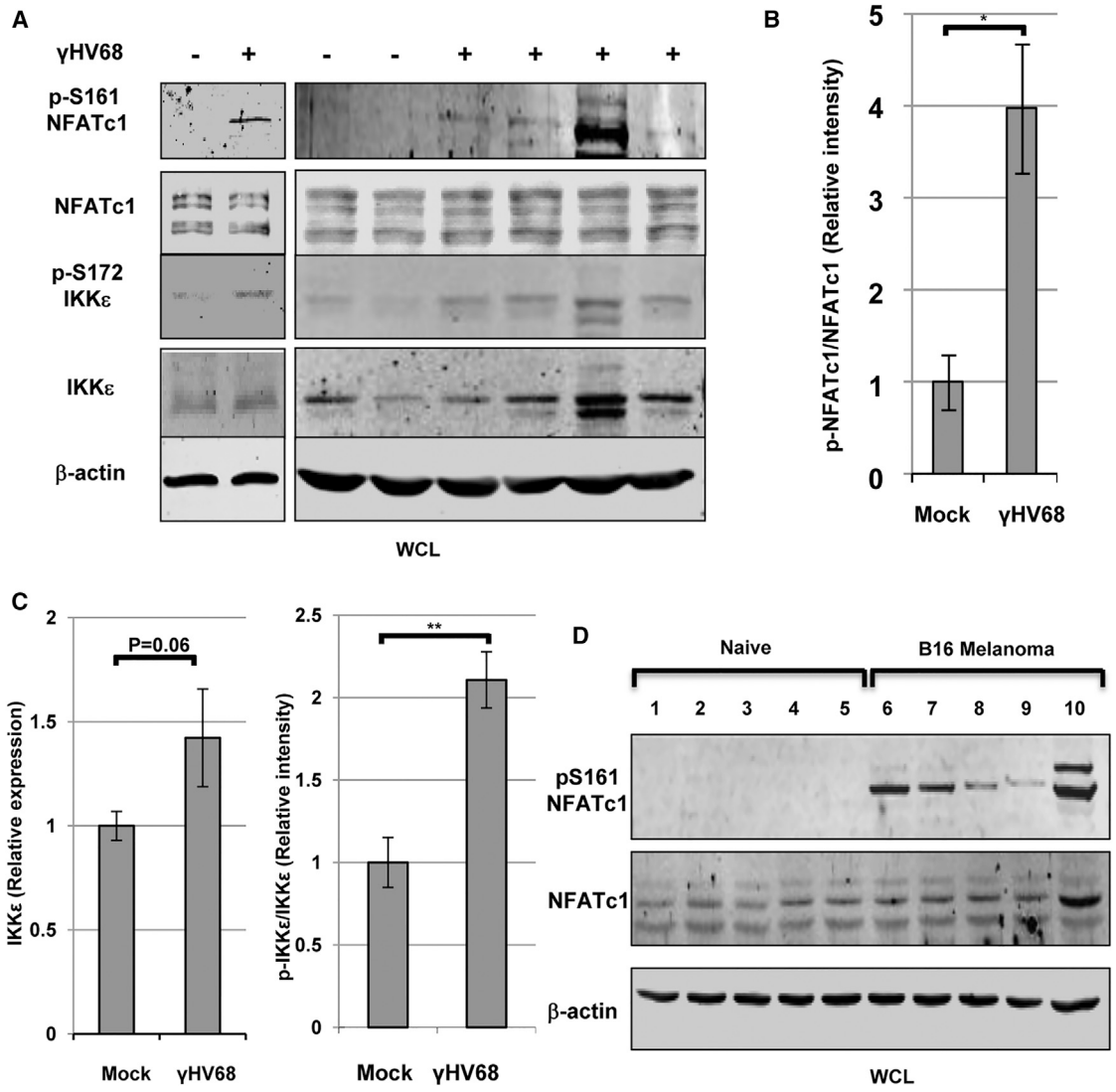

Figure 7. Chronic Activation of IKKε in Persistent Viral Infection and Tumor Development

Age- (12-week-old) and gender-matched mice were infected with γHV68 via intraperitoneal injection, the splenocytes were harvested, and $CD8^+$ T cells were purified.

(A) Whole-cell lysates (WCL) of $CD8^+$ T cells were analyzed by immunoblotting with indicated antibodies.

(B and C) The relative levels of phosphorylated NFATc1 (B), IKKε, and phosphorylated IKKε (C) were determined by densitometry analysis.

(D) Age (12-week-old) and gender-matched mice were inoculated with B16 melanoma cells. Mice were euthanized at 28 dpi, lung $CD8^+$ T cells were collected, and whole-cell lysates were analyzed by immunoblotting.

Error bars denote SD. *$p < 0.05$; **$p < 0.01$.

and 7C). We also examined NFATc1 phosphorylation in a B16 melanoma mouse model. When $CD8^+$ T cells were isolated from lungs of naive mice or mice inoculated with B16 melanoma cells, we observed significantly increased phosphorylation of NFATc1, an indicator of IKKε activation, in mice carrying B16 melanoma cells (Figure 7D). No NFATc1 phosphorylation was detected in $CD8^+$ T cells from naive mice. Collectively, these results support the finding that IKKε is activated in persistent viral infection and tumor-bearing tissue/organs and that activated IKKε phosphorylates NFATc1 to suppress $CD8^+$ T cell immune response.

DISCUSSION

T cells lie in the heart of host defense against chronic immune challenge, such as persisting viral infection and cancer cells. Cytotoxic $CD8^+$ T cells can directly kill virus-infected or -transformed cells, constituting a major arm of adaptive immunity. Upon engagement of the TCR by antigenic peptide-loaded major histocompatibility complex class I (MHC-I), T cells undergo rapid activation and expansion. Central to T cell expansion and ensuing response is the activation of NFAT transcription factors and the expression of genes downstream of NFAT proteins

(Müller and Rao, 2010). Optimal T cell clonal expansion requires an additional co-stimulatory signal from CD28 that is activated by B7 family members (Chen and Flies, 2013). To date, a number of negative regulators are reported to hold T cell activation in check, including NFAT kinases and surface checkpoint molecules, e.g., CTLA-4 and PD-1 (Gibson et al., 2007; Oestreich et al., 2008). Several NFAT kinases, such as GSK3β, casein kinases, and DYRK, can phosphorylate NFAT and inhibit NFAT activation. Although biochemical data established the inhibition of NFAT by these kinases, their roles in T cell activation in vivo remain enigmatic. Interestingly, IL-7-dependent activation of Jak3 in $CD4^{-}CD8^{-}$ double-negative thymocytes was shown to phosphorylate NFATc1 and lead to its nuclear translocation and activation, which is critical for the survival and differentiation of early thymocytes (Patra et al., 2013). IKKε is abundantly expressed in T cells, and its function is not well understood. We report here that IKKε phosphorylates NFATc1 within its N-terminal regulatory domain and inhibits NFAT activation. Upon T cell activation by TCR engagement or calcium influx, IKKε is quickly activated within 10 to 30 min post-stimulation, which is in accordance with a previous report (Peters et al., 2000). Phosphorylation of the Ser^{161} of NFATc1 by IKKε replicates the activation kinetics of IKKε, classifying IKKε as a negative-feedback kinase acting immediately after T cell activation and differentiating IKKε from other NFAT kinases.

Although similar activation kinetics was observed for TBK-1 during T cell activation, knockdown of TBK-1 had no detectable effect on IL-2 expression, even when IKKε expression was depleted. Thus, the closely related TBK-1 and IKKε may have distinct functions in T cells. TBK-1, but not IKKε, was recently shown to modulate neuro-inflammation in $CD4^{+}$ T cells via the AKT-mTORC1 (mammalian target of rapamycin complex 1) signaling pathway (Yu et al., 2015). Our study indicates that the major inhibitory role of IKKε resides in the $CD8^{+}$ T cell compartment. Interestingly, the antibody against γHV68 was not affected by knockout of IKKε, suggesting that the overall function of $CD4^{+}$ T cells is not altered. These results imply that TBK-1 and IKKε may act chiefly in $CD4^{+}$ and $CD8^{+}$ T cells, respectively. Alternatively, IKKε and TBK-1 may play key roles in distinct signaling pathways, e.g., IKKε in NFAT and TBK-1 in AKT pathway. Nevertheless, it remains unknown how IKKε is activated during T cell activation. A recent study reveals that free K48-linked polyubiquitin chains, catalyzed by TRIM6, activate IKKε via promoting oligomerization (Rajsbaum et al., 2014). Whether a similar mechanism of IKKε activation is operating in T cells remains to be determined. The mechanism of IKKε activation, in particular, and its roles in innate immune signaling, in general, in T cells call for investigation.

We provide substantial evidence that IKKε can function as a negative-feedback NFATc1 kinase and restrict T cell activation. IKKε-deficient mice generate a larger number of antiviral and antitumor $CD8^{+}$ effector T cells in vivo. It is noteworthy that NFAT promotes anergy and exhaustion of activated $CD8^{+}$ T cells if not partnered with other transcription factors (e.g., AP-1) (Martinez et al., 2015). Conceivably, depletion of IKKε may elevate these signaling events to promote $CD8^{+}$ T cell activation rather than exhaustion. On the other hand, γHV68 infection and melanoma cells appear to explore the activation of IKKε to restrict antiviral and antitumor $CD8^{+}$ T cell response. Similarly, the $CD8^{+}$ T cell is crucial to control other persistent infectious pathogens, including simian immunodeficiency virus (SIV) infection in rhesus monkey (Schmitz et al., 1999) and hepatitis C virus (HCV) infection in human (Bowen and Walker, 2005; Jo et al., 2009). These results agree well with the established cytotoxic T lymphocyte (CTL) immunity in restricting persistent pathogen infection and chronic cancer development. Despite the robust phenotype of $CD8^{+}$ T cell depletion, these findings implicate the importance of the helper function of $CD4^{+}$ T cells in mounting proper immune response. Previous studies have characterized roles of $CD8^{+}$ and $CD4^{+}$ T cells in EBV- and KSHV-infected patients and in model systems ex vivo (Hislop et al., 2005; Myoung and Ganem, 2011). Conceivably, $CD4^{+}$ T cells are required to activate $CD8^{+}$ T cells that recognize diverse murine γHV68 antigens. Lack of $CD4^{+}$ T cell, as expected, resulted in progressive loss of $CD8^{+}$ T cell function and uncontrolled γHV68 replication (Cardin et al., 1996).

Overall, IKKε promotes NFATc1 phosphorylation during T cell activation, and loss of IKKε robustly elevated the antiviral and antitumor immunity in mice, suggesting that IKKε is a potential immunotherapy target to fight chronic viral infection and cancer.

EXPERIMENTAL PROCEDURES

Viruses, Mice, and Viral Infections

γHV68 was propagated in BHK21 cells as described previously (Feng et al., 2008). IKKε knockout mice (Tenoever et al., 2007), CD45.1 mice, and RAG-2 knockout mice were purchased from Jackson Laboratory. Eight- to 10-week old, gender-matched mice were used for all experiments, unless specified otherwise. All animal work was performed under strict accordance with the recommendations in the Guide for the Care and Use of Laboratory Animals of the NIH. The protocol was approved by the Institutional Animal Care and Use Committee (IACUC) of the University of Southern California. For γHV68 infection, mice were infected with the indicated infectious units of virus in 150 μl of PBS via intranasal or intraperitoneal injection.

$CD8^{+}$ T Cell Depletion

Gender- and age-matched *Ikbke*$^{+/+}$ and *Ikbke*$^{-/-}$ mice were intraperitoneally (i.p.) infected with 1×10^{6} plaque-forming units (PFUs) of γHV68. Mice were mock treated or injected i.p. with purified anti-CD8 antibody (1 mg) (Bio X Cell) at 16 dpi. The depletion was maintained by injecting 1 mg of anti-CD8 antibody every week. Splenocytes were harvested at 42 dpi, and viral genome frequency was determined by limiting-dilution PCR.

Tetramer Staining

γHV68-infected mice were sacrificed at 6, 10, 13, and 42 days post-infection (dpi), and the spleen was collected. Single-cell suspension was generated by passing through a 40-μm strainer on ice. Red blood cells (RBCs) were removed by adding 5 ml of BD Pharm Lyse buffer (BD Biosciences). Cells were washed once with cold PBS plus 1% fetal bovine serum (FBS) and subjected to tetramer staining.

Tetramer staining was carried out as previously described (Molloy et al., 2011). Briefly, cells were incubated with anti-CD16/32 antibody for 10 min on ice, followed by staining for 1 hr in the dark with tetramers. Then, cells were then stained with anti-CD8 antibody for 20 min on ice. Samples were analyzed by flow cytometry using FACSCalibur, and data were analyzed with FlowJo software.

Limiting-Dilution Nested PCR Detection of γHV68 Genome-Positive Cells

The frequency of splenocytes harboring γHV68 genome was measured by limiting-dilution PCR as previously described (Dong et al., 2010). Briefly, mouse spleens were homogenized, re-suspended in isotonic buffer, and subjected to 3-fold serial dilutions (from 10^4 to 41 cells per well) in a background of uninfected RAW 264.7 cells, with a total of 10^4 cells per well. Twelve replicates were plated for each cell dilution. After being plated, cells were subjected to lysis by proteinase K at 56°C for 8 hr. Following inactivation of the enzyme at 85°C for 30 min, samples were subjected to nested PCR using primers specific for γHV68 ORF72. Reaction products were separated using 2.5% UltraPure agarose (Invitrogen) gels and visualized by ethidium bromide staining.

T Cell Adoptive Transfer

T cells of WT (CD45.1) and IKKε-deficient (CD45.2) mice were purified with a $CD8^+$ T cell isolation kit (Miltenyi Biotec). Two million T cells were combined and transferred intravenously (i.v.) into RAG2-deficient mice. At 16 hr after adoptive transfer, RAG2-deficient mice were infected with 10^6 PFU of γHV68. Splenocytes were collected at 13 dpi and analyzed by flow cytometry with antibodies against CD8, CD45.1, and CD45.2.

T cells from IKKε-deficient (CD45.2) mice were purified with a $CD8^+$ T cell isolation kit (Miltenyi Biotec), and 3 million of the purified $CD8^+$ T cells were injected i.v. into WT mice (CD45.1). Mice were then challenged with 10^6 PFU of γHV68 (i.p.). Mice were euthanized at 16 dpi, and splenocytes were collected and analyzed by flow cytometry with antibodies against CD8, CD45.1, CD45.2, and virus-specific tetramer.

Melanoma Development in Mice

Mice were injected i.v. with B16.MO5 (MO5) melanoma cells expressing the ovalbumin (OVA) antigen (2×10^5) and euthanized at the indicated time. Melanoma tumors in the lung were enumerated. The entire lung was minced and digested with collagenase. T cells were analyzed by flow cytometry with antibodies against CD8, CD44, PD-1, and OVA tetramer (SIINFEKL).

Statistical Analysis

Data represent the mean of three independent experiments, and error bars denote SD unless specified otherwise. A two-tailed Student's t test was used for statistical analysis. The mouse Kaplan-Meier survival curve was generated using GraphPad 5, and the log-rank test applied to the mouse survival data was also performed in GraphPad 5.

ACCESSION NUMBERS

The accession number for the data reported in this paper is GEO: GSE79074.

SUPPLEMENTAL INFORMATION

Supplemental Information includes Supplemental Experimental Procedures and seven figures and can be found with this article online at http://dx.doi.org/10.1016/j.celrep.2016.05.083.

AUTHOR CONTRIBUTIONS

J. Zhang and P.F. conceived the study. J. Zhang, H.F., E.R.F., S.A.T., and P.F. performed the experiments. All authors contributed to experimental design and data analysis. J. Zhang and P.F. prepared the manuscript. All authors read and approved the manuscript.

ACKNOWLEDGMENTS

We thank Drs. Eric Olson and Yousang Gwack for providing plasmids; Steve Gygi, Ross Tomaino, Yu Zhou, and Ebrahim Zandi for mass spectrometry analysis; Roger Davis, Chi-Wing Chow, and Takeshi Saito for antibody; Adolfo Garcia-Sastre and Xue Huang for advice regarding mouse experiments; and Ms. Lillian Young for H&E staining. We thank Dr. Lin Chen and other members of the P.F. lab for their comments. We thank the NIH Tetramer Core Facility (Emory University) to provide the $H2K^b$ tetramer against ORF61 and OVA. This work is supported by grants from the NIDCR (DE021445 and DE026003), NCI (CA180779), the Wright Foundation, the Margaret E. Early Research Trust, and ACS (RSG-11-162-01-MPC) to P.F. and from the Natural Science Foundation of China (NSFC 81471963) to H.F.

Received: December 15, 2015
Revised: March 11, 2016
Accepted: May 19, 2016
Published: June 23, 2016

REFERENCES

Boehm, J.S., Zhao, J.J., Yao, J., Kim, S.Y., Firestein, R., Dunn, I.F., Sjostrom, S.K., Garraway, L.A., Weremowicz, S., Richardson, A.L., et al. (2007). Integrative genomic approaches identify IKBKE as a breast cancer oncogene. Cell *129*, 1065–1079.

Bowen, D.G., and Walker, C.M. (2005). Adaptive immune responses in acute and chronic hepatitis C virus infection. Nature *436*, 946–952.

Bulek, K., Liu, C., Swaidani, S., Wang, L., Page, R.C., Gulen, M.F., Herjan, T., Abbadi, A., Qian, W., Sun, D., et al. (2011). The inducible kinase IKKi is required for IL-17-dependent signaling associated with neutrophilia and pulmonary inflammation. Nat. Immunol. *12*, 844–852.

Cardin, R.D., Brooks, J.W., Sarawar, S.R., and Doherty, P.C. (1996). Progressive loss of CD8+ T cell-mediated control of a gamma-herpesvirus in the absence of CD4+ T cells. J. Exp. Med. *184*, 863–871.

Chen, L., and Flies, D.B. (2013). Molecular mechanisms of T cell co-stimulation and co-inhibition. Nat. Rev. Immunol. *13*, 227–242.

Chow, C.W., Rincón, M., Cavanagh, J., Dickens, M., and Davis, R.J. (1997). Nuclear accumulation of NFAT4 opposed by the JNK signal transduction pathway. Science *278*, 1638–1641.

Chow, C.W., Rincón, M., and Davis, R.J. (1999). Requirement for transcription factor NFAT in interleukin-2 expression. Mol. Cell. Biol. *19*, 2300–2307.

Chuvpilo, S., Avots, A., Berberich-Siebelt, F., Glöckner, J., Fischer, C., Kerstan, A., Escher, C., Inashkina, I., Hlubek, F., Jankevics, E., et al. (1999). Multiple NF-ATc isoforms with individual transcriptional properties are synthesized in T lymphocytes. J. Immunol. *162*, 7294–7301.

Chuvpilo, S., Jankevics, E., Tyrsin, D., Akimzhanov, A., Moroz, D., Jha, M.K., Schulze-Luehrmann, J., Santner-Nanan, B., Feoktistova, E., König, T., et al. (2002). Autoregulation of NFATc1/A expression facilitates effector T cells to escape from rapid apoptosis. Immunity *16*, 881–895.

Doherty, P.C., Christensen, J.P., Belz, G.T., Stevenson, P.G., and Sangster, M.Y. (2001). Dissecting the host response to a gamma-herpesvirus. Philos. Trans. R. Soc. Lond. B Biol. Sci. *356*, 581–593.

Dong, X., Feng, H., Sun, Q., Li, H., Wu, T.T., Sun, R., Tibbetts, S.A., Chen, Z.J., and Feng, P. (2010). Murine gamma-herpesvirus 68 hijacks MAVS and IKKbeta to initiate lytic replication. PLoS Pathog. *6*, e1001001.

Feng, H., Dong, X., Negaard, A., and Feng, P. (2008). Kaposi's sarcoma-associated herpesvirus K7 induces viral G protein-coupled receptor degradation and reduces its tumorigenicity. PLoS Pathog. *4*, e1000157.

Fitzgerald, K.A., McWhirter, S.M., Faia, K.L., Rowe, D.C., Latz, E., Golenbock, D.T., Coyle, A.J., Liao, S.M., and Maniatis, T. (2003). IKKepsilon and TBK1 are essential components of the IRF3 signaling pathway. Nat. Immunol. *4*, 491–496.

Gibson, H.M., Hedgcock, C.J., Aufiero, B.M., Wilson, A.J., Hafner, M.S., Tsokos, G.C., and Wong, H.K. (2007). Induction of the CTLA-4 gene in human lymphocytes is dependent on NFAT binding the proximal promoter. J. Immunol. *179*, 3831–3840.

Greenblatt, M.B., Aliprantis, A., Hu, B., and Glimcher, L.H. (2010). Calcineurin regulates innate antifungal immunity in neutrophils. J. Exp. Med. *207*, 923–931.

Gulen, M.F., Bulek, K., Xiao, H., Yu, M., Gao, J., Sun, L., Beurel, E., Kaidanovich-Beilin, O., Fox, P.L., DiCorleto, P.E., et al. (2012). Inactivation of the enzyme GSK3α by the kinase IKKi promotes AKT-mTOR signaling pathway

that mediates interleukin-1-induced Th17 cell maintenance. Immunity *37*, 800–812.

Guo, J.P., Shu, S.K., He, L., Lee, Y.C., Kruk, P.A., Grenman, S., Nicosia, S.V., Mor, G., Schell, M.J., Coppola, D., and Cheng, J.Q. (2009). Deregulation of IKBKE is associated with tumor progression, poor prognosis, and cisplatin resistance in ovarian cancer. Am. J. Pathol. *175*, 324–333.

Hislop, A.D., Kuo, M., Drake-Lee, A.B., Akbar, A.N., Bergler, W., Hammerschmitt, N., Khan, N., Palendira, U., Leese, A.M., Timms, J.M., et al. (2005). Tonsillar homing of Epstein-Barr virus-specific CD8+ T cells and the virus-host balance. J. Clin. Invest. *115*, 2546–2555.

Horsley, V., Aliprantis, A.O., Polak, L., Glimcher, L.H., and Fuchs, E. (2008). NFATc1 balances quiescence and proliferation of skin stem cells. Cell *132*, 299–310.

Hutti, J.E., Shen, R.R., Abbott, D.W., Zhou, A.Y., Sprott, K.M., Asara, J.M., Hahn, W.C., and Cantley, L.C. (2009). Phosphorylation of the tumor suppressor CYLD by the breast cancer oncogene IKKepsilon promotes cell transformation. Mol. Cell *34*, 461–472.

Jo, J., Aichele, U., Kersting, N., Klein, R., Aichele, P., Bisse, E., Sewell, A.K., Blum, H.E., Bartenschlager, R., Lohmann, V., and Thimme, R. (2009). Analysis of CD8+ T-cell-mediated inhibition of hepatitis C virus replication using a novel immunological model. Gastroenterology *136*, 1391–1401.

Mancini, M., and Toker, A. (2009). NFAT proteins: emerging roles in cancer progression. Nat. Rev. Cancer *9*, 810–820.

Martinez, G.J., Pereira, R.M., Äijö, T., Kim, E.Y., Marangoni, F., Pipkin, M.E., Togher, S., Heissmeyer, V., Zhang, Y.C., Crotty, S., et al. (2015). The transcription factor NFAT promotes exhaustion of activated CD8$^+$ T cells. Immunity *42*, 265–278.

Molloy, M.J., Zhang, W., and Usherwood, E.J. (2011). Suppressive CD8+ T cells arise in the absence of CD4 help and compromise control of persistent virus. J Immunol. *186*, 6218–6226.

Muhammad, K., Alrefai, H., Marienfeld, R., Pham, D.A., Murti, K., Patra, A.K., Avots, A., Bukur, V., Sahin, U., Kondo, E., et al. (2014). NF-κB factors control the induction of NFATc1 in B lymphocytes. Eur. J. Immunol. *44*, 3392–3402.

Müller, M.R., and Rao, A. (2010). NFAT, immunity and cancer: a transcription factor comes of age. Nat. Rev. Immunol. *10*, 645–656.

Müller, M.R., Sasaki, Y., Stevanovic, I., Lamperti, E.D., Ghosh, S., Sharma, S., Gelinas, C., Rossi, D.J., Pipkin, M.E., Rajewsky, K., et al. (2009). Requirement for balanced Ca/NFAT signaling in hematopoietic and embryonic development. Proc. Natl. Acad. Sci. USA *106*, 7034–7039.

Myoung, J., and Ganem, D. (2011). Active lytic infection of human primary tonsillar B cells by KSHV and its noncytolytic control by activated CD4+ T cells. J. Clin. Invest. *121*, 1130–1140.

Oestreich, K.J., Yoon, H., Ahmed, R., and Boss, J.M. (2008). NFATc1 regulates PD-1 expression upon T cell activation. J. Immunol. *181*, 4832–4839.

Okoye, I., Wang, L., Pallmer, K., Richter, K., Ichimura, T., Haas, R., Crouse, J., Choi, O., Heathcote, D., Lovo, E., et al. (2015). T cell metabolism. The protein LEM promotes CD8$^+$ T cell immunity through effects on mitochondrial respiration. Science *348*, 995–1001.

Patra, A.K., Avots, A., Zahedi, R.P., Schüler, T., Sickmann, A., Bommhardt, U., and Serfling, E. (2013). An alternative NFAT-activation pathway mediated by IL-7 is critical for early thymocyte development. Nat. Immunol. *14*, 127–135.

Peters, R.T., Liao, S.M., and Maniatis, T. (2000). IKKepsilon is part of a novel PMA-inducible IkappaB kinase complex. Mol. Cell *5*, 513–522.

Rajsbaum, R., Versteeg, G.A., Schmid, S., Maestre, A.M., Belicha-Villanueva, A., Martínez-Romero, C., Patel, J.R., Morrison, J., Pisanelli, G., Miorin, L., et al. (2014). Unanchored K48-linked polyubiquitin synthesized by the E3-ubiquitin ligase TRIM6 stimulates the interferon-IKKε kinase-mediated antiviral response. Immunity *40*, 880–895.

Reilly, S.M., Chiang, S.H., Decker, S.J., Chang, L., Uhm, M., Larsen, M.J., Rubin, J.R., Mowers, J., White, N.M., Hochberg, I., et al. (2013). An inhibitor of the protein kinases TBK1 and IKK-ε improves obesity-related metabolic dysfunctions in mice. Nat. Med. *19*, 313–321.

Rudolf, R., Busch, R., Patra, A.K., Muhammad, K., Avots, A., Andrau, J.C., Klein-Hessling, S., and Serfling, E. (2014). Architecture and expression of the nfatc1 gene in lymphocytes. Front. Immunol. *5*, 21.

Schmitz, J.E., Kuroda, M.J., Santra, S., Sasseville, V.G., Simon, M.A., Lifton, M.A., Racz, P., Tenner-Racz, K., Dalesandro, M., Scallon, B.J., et al. (1999). Control of viremia in simian immunodeficiency virus infection by CD8+ lymphocytes. Science *283*, 857–860.

Serfling, E., Chuvpilo, S., Liu, J., Höfer, T., and Palmetshofer, A. (2006). NFATc1 autoregulation: a crucial step for cell-fate determination. Trends Immunol. *27*, 461–469.

Sharma, S., tenOever, B.R., Grandvaux, N., Zhou, G.P., Lin, R., and Hiscott, J. (2003). Triggering the interferon antiviral response through an IKK-related pathway. Science *300*, 1148–1151.

Shen, R.R., Zhou, A.Y., Kim, E., Lim, E., Habelhah, H., and Hahn, W.C. (2012). IκB kinase ε phosphorylates TRAF2 to promote mammary epithelial cell transformation. Mol. Cell. Biol. *32*, 4756–4768.

Shimada, T., Kawai, T., Takeda, K., Matsumoto, M., Inoue, J., Tatsumi, Y., Kanamaru, A., and Akira, S. (1999). IKK-i, a novel lipopolysaccharide-inducible kinase that is related to IkappaB kinases. Int. Immunol. *11*, 1357–1362.

Tenoever, B.R., Ng, S.L., Chua, M.A., McWhirter, S.M., García-Sastre, A., and Maniatis, T. (2007). Multiple functions of the IKK-related kinase IKKepsilon in interferon-mediated antiviral immunity. Science *315*, 1274–1278.

Xie, X., Zhang, D., Zhao, B., Lu, M.K., You, M., Condorelli, G., Wang, C.Y., and Guan, K.L. (2011). IkappaB kinase epsilon and TANK-binding kinase 1 activate AKT by direct phosphorylation. Proc. Natl. Acad. Sci. USA *108*, 6474–6479.

Yu, J., Zhou, X., Chang, M., Nakaya, M., Chang, J.H., Xiao, Y., Lindsey, J.W., Dorta-Estremera, S., Cao, W., Zal, A., et al. (2015). Regulation of T-cell activation and migration by the kinase TBK1 during neuroinflammation. Nat. Commun. *6*, 6074.

Zanoni, I., Ostuni, R., Capuano, G., Collini, M., Caccia, M., Ronchi, A.E., Rocchetti, M., Mingozzi, F., Foti, M., Chirico, G., et al. (2009). CD14 regulates the dendritic cell life cycle after LPS exposure through NFAT activation. Nature *460*, 264–268.

Zhang, J., He, S., Wang, Y., Brulois, K., Lan, K., Jung, J.U., and Feng, P. (2015). Herpesviral G protein-coupled receptors activate NFAT to induce tumor formation via inhibiting the SERCA calcium ATPase. PLoS Pathog. *11*, e1004768.